www.czasopisma.pan.pl PAN POLSKA AKADEMIA NAUK www.journals.pan.pl

A R C H I V E S O F M E T A L L U R G Y A N D M A T E R I A L S

Volume 60 2015 Issue 4

DOI: 10.1515/amm-2015-0445

A. BOKOTA*#, A. KULAWIK*, R. SZYMCZYK*, J. WRÓBEL*

THE NUMERICAL ANALYSIS OF THE PHENOMENA OF SUPERFICIAL HARDENING OF THE HOT-WORK TOOL STEEL ELEMENTS

ANALIZA NUMERYCZNA ZJAWISK PRZYPOWIERZCHNIOWEGO HARTOWANIA ELEMENTÓW ZE STALI NARZĘDZIOWEJ DO PRACY NA GORĄCO

In the paper the complex model of hardening of the hot-work tool steel is presented. Model of estimation of phase fractions and their kinetics is based on the continuous heating diagram (CHT) and cooling diagram (CCT). Phase fractions which occur during the continuous heating and cooling (austenite, pearlite or bainite) are described by Johnson-Mehl (JM) formula. To determine of the formed martensite the modified Koistinen-Marburger (KM) equation is used. Model takes into account the thermal, structural, plastic strains and transformation plasticity. To calculate the plastic strains the Huber-Mises plasticity condition with isotopic hardening is used. Whereas to determine transformations induced plasticity the Leblond model is applied. The numerical analysis of phase compositions and residual stresses in the hot-work steel (W360) element is considered.

Keywords: heat treatment, hot-work tool steel, phase transformations, stress, thermo-elastic-plastic finite element analysis

W pracy przedstawiono kompleksowy model hartowania stali narzędziowej do pracy na gorąco. Model szacowania ułamków faz oraz ich kinetyki oparto na wykresach ciągłego nagrzewania (CTP_A) oraz chłodzenia (CTPc). Ułamki faz powstałych podczas ciągłego nagrzewania i chłodzenia (austenit, perlit lub bainit) wyznaczane są równaniem Johnsona-Mehla. Do określenia tworzącego się martenzytu wykorzystano zmodyfikowane równanie Koistinena i Marburgera. W modelu uwzględniono odkształcenia cieplne, strukturalne, plastyczne oraz odkształcenia transformacyjne. Do wyznaczania odkształceń plastycznych zastosowano warunek plastyczności Hubera-Misesa ze wzmocnieniem izotropowym, natomiast do wyznaczenia odkształceń transformacyjnych wykorzystano model Leblonda. Dokonano analizy numerycznej składu fazowego oraz naprężeń hartowniczych w elementach wykonanych ze stali narzędziowej do pracy na gorąco (W360).

1. Introduction

The heat treatment of hot-work tool steel is a technological process, in which thermal phenomena, phase transformations and mechanical phenomena are dominant. Models, which describe processes mentioned above, don't take into consideration the many important aspects. As a result of the complexity of phenomenon of heat treatment process, there are many mathematical and numerical difficulties in its modelling. For this reason there hasn't a model which includes phenomenon accompanying heat treatment and hardening of hot-work tool steel [1-6].

The numerical analysis of the heat treatment processes is the important problem for the modern lab which designs for the industry. The special attention on the development this branch of the numerical methods is inspired by the industry, which due to the modern technology and reduces the cost, requires the tools to improve the heat treatment processes. The research works including the issue of the heat treatment can be divided into those that in the complex way analyze the presented phenomena, as well as those that focus only on the one phenomena of the heat treatment process. The phenomena occurring during the heat treatment are very complex and still incompletely described. The model of the hardening process should contain at least with three coupling elements: thermal, structural and mechanical [3,4,7-11]. Determination of the composition of each phases, their kinetics and obtained structures during the cooling process of iron alloys is necessary to calculate the stresses for the hardening process. In the heat treatment process the significant stresses are generated and cause, in most cases, the plasticize of the material. Therefore, in the modeling of mechanical phenomena the use of the models of elastic-plastic materials is required. Additionally, to ensure the reliability of the results of numerical simulations of mechanical phenomena, except thermal, structural and plastic strains the transformation induced plasticity should be taken into account [3,12-18].

* CZESTOCHOWA UNIVERSITY OF TECHNOLOGY, INSTITUTE OF COMPUTER AND INFORMATION SCIENCES, THE FACULTY OF MECHANICAL ENGINEERING AND COMPUTER SCIENCE, 73 DĄBROWSKIEGO STR., 42-200 CZESTOCHOWA, POLAND

Corresponding author: bokota@icis.pcz.pl

The element which has the significant influence on the results of numerical simulation of the hardening is the appropriate choice of the cooling conditions which are modeled by the boundary conditions. This is important in the case of quenching the hot-work tool steel, which is easily hardened [6]. Therefore, in the paper paid attention to this problem by comparing the results from numerical simulation for the two rate of cooling, although both are relatively small. To implement this type of algorithms one usually applies the FEM, which makes it possible to take into account both nonlinearities and inhomogeneity of thermally processed material [1,3,10,13,19,20].

2. Model of heat transfer phenomena

The fields of temperature are determined from heat transfer equation:

$$\operatorname{div}(\lambda \operatorname{grad}(T)) - C\frac{\partial T}{\partial t} = -Q,\ T = T(x_\alpha, t) \tag{1}$$

where $\lambda=\lambda(T)$ is the heat conductivity coefficient [W/(mK)], $T=T(x_\alpha t)$ temperature [K], $C=C(T)$ is an effective heat capacity [J/(m^{3}K)], Q is intensity of internal sources in which the heat of phase transformations are taken into account [W/m^3], x_α are the coordinates [m] and t is time [s].

The equation (1) is supplemented by initial conditions

$$T(x_\alpha, t_0) = T_0(x_\alpha),\ \ Q(x_\alpha, t_0) = Q_0(x_\alpha) = 0 \tag{2}$$

and boundary conditions:

a) On the part of the edge $\Gamma = \Gamma_q$ the heat flux is given $q=q^*$, Neumann condition (type II). A condition of this type the thermal insulation is modeled.

$$-\lambda\frac{\partial T}{\partial n}\bigg|_\Gamma = q_n = 0 \tag{3}$$

b) On the part of the edge $\Gamma = \Gamma_\infty$ the heat flux (q_n) is determined by the difference between the temperature of edge and the surrounding medium, Newton condition (type III). In the paper by this type of boundary condition the heating and cooling process is modeled.

$$-\lambda\frac{\partial T}{\partial n}\bigg|_{\Gamma_\infty} = q_n = \alpha(T)\left(T\big|_\Gamma - T_\infty\right) \tag{4}$$

where $\alpha(T)$ is the heat transfer coefficient [W/(m^{2}K)], Γ is surface, from which the heat is taken over, T_∞ is temperature of the medium rounded.

Heat of phase transformations $\left(Q^{ph}\right)$ take into account in source unit of conductivity equation (1) calculate by formula [3,10,21]:

$$Q = \dot{Q}^{ph} = \sum_k \dot{Q}_k^{\eta_k} = \sum_k H_k^{\eta_k}\dot{\eta}_k \tag{5}$$

where: $H_k^{\eta_k}$ is volumetric heat of k - phase transformations [J/m^3] (k=2..5 appropriate for the bainite, ferrite, martensite and pearlite), $\dot{\eta}_k$ is rate of change fractions of k - phase.

This internal heat source could be taken into account by enthalpy changes. The following enthalpy changes for the diffusional and diffusionless transformations were used [11,21]:

$$\Delta H_B = 314\times10^6,\ \Delta H_M = 630\times10^6,\ \Delta H_P = 800\times10^6 \tag{6}$$

where ΔH_B, ΔH_M and ΔH_P indicate the enthalpy changes during austenite-bainite, austenite-martensite and austenite-pearlite transformations, respectively.

To solve, presented above, the heat transfer phenomena, i.e. heat transfer equation (1) with completed initial (2) and boundary conditions (3), (4), the finite element method in Galerkin formulation was used [3,22].

3. Model of phase transformations in the solid state

In the paper the macroscopic model for calculation of the created fractions of the phases in solid state, for hot-work tool steel (W360), is used for following chemical composition (Table 1) [6]:

TABLE 1

The chemical composition of the considered steel (W360)

Steel	C%	Mn%	Si%	Cr%	Mo%	V%
W360	0.50	0.25	0.20	4.50	3.00	0.55

The continuous cooling diagram (CCT) is used to determine the significant parameters of phase transformations model (the time and the temperature of start and end of transformations) (Fig. 1) [6].

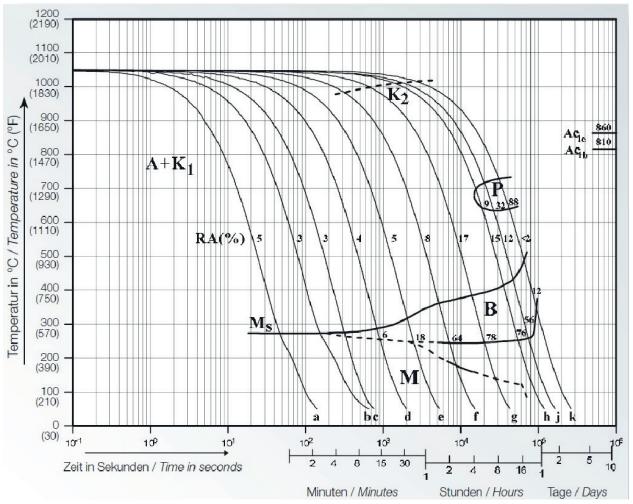

Fig. 1. The Continuous Cooling Transformation diagram (CCT) for the hot-work tool steel W360 [6]

To calculate the kinetic of phase transformation of heating (transformation to austenite) the diagram of continuous heating (CHT) is used. Whereas to determine the phase transformations in the cooling process the new defined diagram of continuous

cooling (CCT) for the higher temperature of austenitization (offset CCT diagram) are taken into account (Fig. 2). The offset of the diagram to the left side, in reference to the original graph (Fig. 1), is the result of the changes in method of CCT diagram analysis. It was assumed that the start point of cooling curve is in the point of intersection of the two lines - cooling curve and the temperature line in 800°C. In this way can avoid, in the simulation of the kinetic of cooling transformations, the offset all lines on the CCT diagram for the different heating temperatures [6].

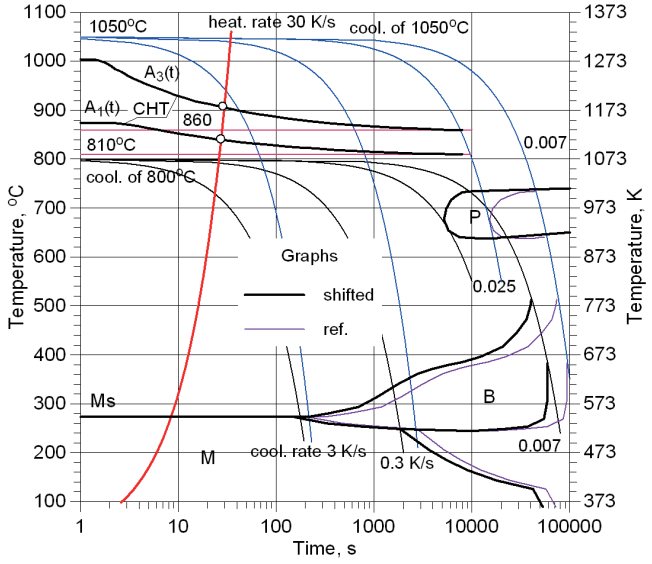

Fig. 2. The Continuous Cooling Transformation diagram (CHT) and shifted CCT diagram with marked cooling rate for the hot-work tool steel W360

The kinetics of phase transformation in solid state i.e. during heating process - austenitization, cooling - austenite to pearlite or bainite in model are calculated by JM formula. The changes of content of martensite are defined by the empirical KM equation [3,13,23,24]:

$$\begin{aligned}
&\tilde{\eta}_A(T,t) = 1-\exp(-b(t_s,t_f)(t^{n(t_s,t_f)}(T)), \text{ heating}\\
&\eta_{BFP}(T,t) = \eta_m\left(1-\exp\left(-b\left(t^n(T)\right)\right)\right), \text{ cooling}\\
&\eta_M(T) = \eta_m\left(1-\exp\left(-\left((M_s-T)/(M_s-M_f)\right)^m\right)\right), \text{ cooling}
\end{aligned} \quad (7)$$

where
$\eta_m = \eta^{\%}_{(.)}\tilde{\eta}_A$ for $\tilde{\eta}_A \geq \eta^{\%}_{(.)}$ and $\eta_m = \tilde{\eta}_A$ for $\tilde{\eta}_A < \eta^{\%}_{(.)}$, $\eta^{\%}_{(.)}$ is maximal phase fraction for established cooling rate estimated on the basis of CCT diagram, $b(t_s,t_f)$ and $n(t_s,t_f)$ are coefficients calculated assuming the initial fraction ($\eta_s(t_s)$=0.01) and the maximum value of fraction ($\eta_f(t_f)$=0.99), $\tilde{\eta}_A$ is the fraction of forming austenite after heating, m is a constant from experiment; for considered steel m = 3.5, the start temperature of martensite transformation amount M_s=548 K, and final temperature of transformation is equal M_f=123 K [14,16].

Increases of the isotropic deformation $\left(\dot{\varepsilon}^{Tph}\right)$ caused by changes of the temperature and phase transformation in the heating and cooling processes are calculated using the following relations for heating and cooling respectively[3,10]:

$$\dot{\varepsilon}^{Tph} = \dot{\varepsilon}^{Tph}_H = \sum_{k=1}^{k=5}\alpha_k\eta_k\dot{T} - \varepsilon^{ph}_A\dot{\eta}_A,\ \dot{\varepsilon}^{Tph} = \dot{\varepsilon}^{Tph}_C = \sum_{k=1}^{k=5}\alpha_k\eta_k\dot{T} + \sum_{k=2}^{k=5}\varepsilon^{ph}_k\dot{\eta}_k \quad (8)$$

where $\alpha_k = \alpha_k(T)$ are coefficients of thermal expansion of: austenite, bainite, ferrite, martensite and pearlite, respectively, ε^{ph}_A is the isotropic deformation accompanying transformation of the input structure into austenite, whereas ε^{ph}_A are isotropic deformations from phase transformation of: austenite into bainite, ferrite, martensite, or of austenite into pearlite, respectively.

For the considered steel, the values of thermal expansion coefficients for the initial structure (spheroid), described in the articles, have the values depend on the temperature: 100°C - 11.1×10^{-6} 1/K, 400°C - 12.3×10^{-6} 1/K and 700°C - 13.6×10^{-6} 1/K. The thermal expansion coefficient for the austenite is equal 22×10^{-6} 1/K [6].

Therefore, that the thermal expansion coefficient is not a line function, it is approximated by square function, which passed through the points described above:

$$\alpha_{FP}(T) = 5.5556\times10^{-13}T^2 + 3.4189\times10^{-9}T + 9.7475\cdot10^{-6} \quad (9)$$

Isotropic structural strains are calculated on the base of literature review and analysis of numerical dilatometric tests obtained for different cooling rate. These tests are made for the large range of cooling rate for the austenite to pearlite, to bainite and to martensite transformations. The values of structural strain coefficient are equal: 2.2, 6.0, 8.2 and 2.85 ($\times10^{-3}$) for austenite, bainite, martensite and pearlite respectively [6,10].

The comparison of results from the simulation of cooling process with different established cooling rate (the average cooling rate in the range of 800 - 500°C (see Fig. 2)) is presented on the figure 3. To calculate the dilatometric curve the equation (8) is used. The displacement on figure 3 are referred to base length equal 10 mm (most applied length of the dilatometric specimen).

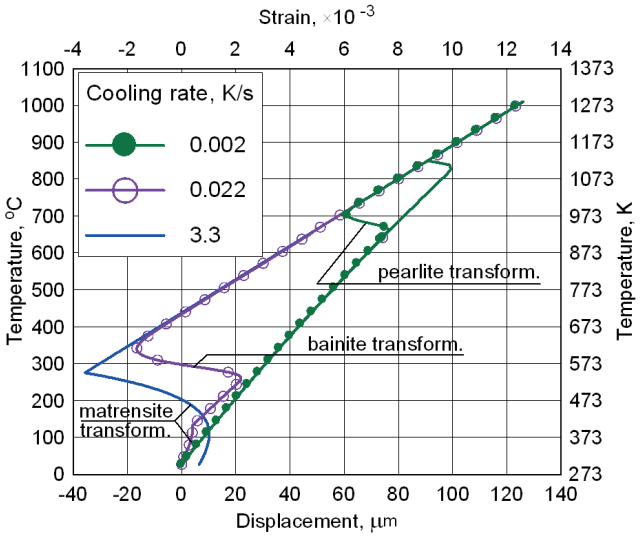

Fig. 3. Calculate dilatometric curves for established cooling rate (see Fig. 2)

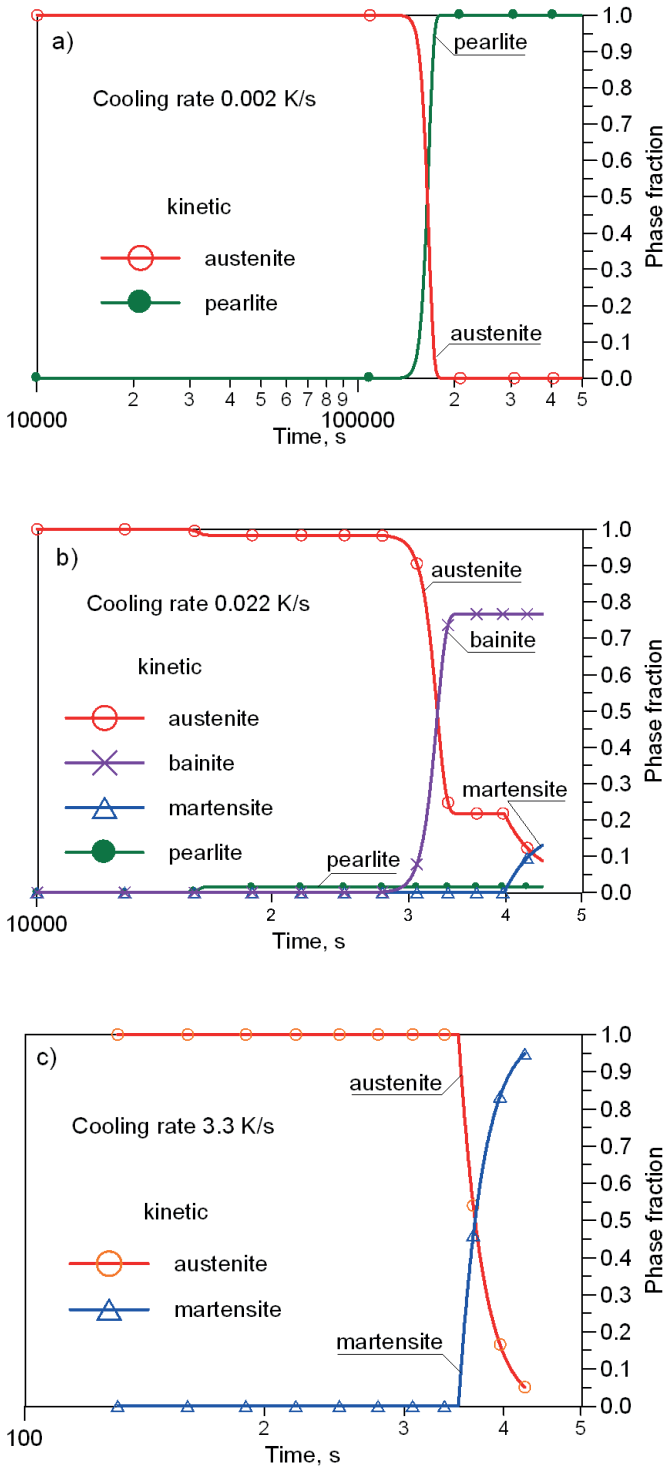

Fig. 4. Kinetic of transformations for cooling rate - a) 0.002, b) 0.022 and c) 3.3 K/s (see Fig. 2)

The analysis of simulation results of phase transformation kinetics of the W360 steel showed that the martensite structure was obtained already for the cooling rate equal 3 K/s. This cooling process takes much more time in comparison to required time for cooling process of the carbon tool steel element [6,8,10]. Therefore, that the required structure after hardening process is the microstructure of martensite and bainite, the cooling rate should be much less than 3 K/s (Fig. 4).

4. Model of thermo-elasto-plastic stress and strain

The stresses and strains are calculated by the solution of equilibrium equations and constitutive relations in the rate form, i.e.:

$$\mathrm{div}\dot{\boldsymbol{\sigma}}(x_\alpha,t)=\mathbf{0},\ \dot{\boldsymbol{\sigma}}=\dot{\boldsymbol{\sigma}}^T,\ \dot{\boldsymbol{\sigma}}=\mathbf{D}\circ\dot{\boldsymbol{\varepsilon}}^{\mathrm{e}}+\dot{\mathbf{D}}\circ\boldsymbol{\varepsilon}^{\mathrm{e}} \tag{10}$$

where $\boldsymbol{\sigma}=\boldsymbol{\sigma}(\sigma_{\alpha\beta})$ is stress tensor, $\mathbf{D}=\mathbf{D}(v,E)$ is the tensor of material constants (isotropic materials), v, is Poisson ratio, $E=E(T)$ is the Young's modulus, however $\boldsymbol{\varepsilon}^e$ is tensor elastic strains.

The equation (10) is completed by initial conditions

$$\boldsymbol{\sigma}(x_\alpha,t_0)=\mathbf{0},\ \boldsymbol{\varepsilon}^{\mathrm{e}}(x_\alpha,t_0)=\mathbf{0},\ t_0=0 \tag{11}$$

and boundary conditions which provide external statically determinate

$$\dot{\mathbf{U}}(x_\alpha,t)\big|_\Gamma=\bar{\dot{\mathbf{U}}},\ \left(\bar{\dot{\mathbf{U}}}=\mathbf{0}\right) \tag{12}$$

where $\mathbf{U}$ is the vector of displacement, $\bar{\dot{\mathbf{U}}}$ - remove degrees of freedom.

Total strains in the around considered points are result of the sum (assumed the rule of additivity of strain):

$$\boldsymbol{\varepsilon}=\boldsymbol{\varepsilon}^{e}+\boldsymbol{\varepsilon}^{Tph}+\boldsymbol{\varepsilon}^{tp}+\boldsymbol{\varepsilon}^{p} \tag{13}$$

where $\boldsymbol{\varepsilon}^{Tph}$ are isotrope of temperature and structural strains, $\boldsymbol{\varepsilon}^{tp}$ are transformations plasticity, and $\boldsymbol{\varepsilon}^{p}$ are plastic strains.

For the Huber-Misses plasticity condition the flow function (f) has the form [3,8,10,13]:

$$f=\sigma_{ef}-Y\left(T,\sum Y_0^k(T)\eta_k,\varepsilon_{ef}^{\mathrm{p}}\right)=0,\ Y_0=\sum Y_0^k(T)\eta_k,\ k=1...5 \tag{14}$$

where σ_{ef} is effective stress, $\varepsilon_{ef}^{\mathrm{p}}$ is effective plastic strain, Y is a plasticized stress of material on the phase fraction ($\Sigma\eta_k$) in temperature (T) and effective strain (ε_{ef}^{p}):

$$Y\left(T,\sum Y_0^k(T)\eta_k,\varepsilon_{ef}^{\mathrm{p}}\right)=Y_0\left(T,\sum\eta_k\right)+Y_H\left(T,\varepsilon_{ef}^{p}\right),\ Y_0\left(T,\sum\eta_k\right)=\sum Y_0^k(T)\eta_k \tag{15}$$

$Y_0\left(T,\sum\eta_k\right)$ is a yield points of material dependent on the temperature and the phase fraction, however $Y_H=Y_H\left(T,\varepsilon_{ef}^{p}\right)$ is a surplus of the stress resulting from the material hardening

$Y_H=Y_H\left(T,\varepsilon_{ef}^{p}\right)=Y_H\left(\kappa(T),\varepsilon_{ef}^{p}\right)$

wherein the $\kappa=\kappa(T)$ is the hardening modulus.

The plastic strains is determined by nonisothermic plastic flow law [3, 11,22]:

$$\dot{\boldsymbol{\varepsilon}}^{\mathrm{p}}=\dot{\varepsilon}_{ef}^{p}\frac{\partial f}{\partial\boldsymbol{\sigma}},\quad \dot{f}=0,\quad \dot{\boldsymbol{\varepsilon}}^{\mathrm{p}}=\dot{\varepsilon}_{ef}^{p}\frac{3\mathbf{S}}{2Y} \tag{16}$$

where **S** is the deviatoric part of stress tensor (**S**=**σ**–**I**σ_{kk}/3).

Using the Leblond model, completed by decreasing functions $(1-\eta)$ which has been proposed by the authors of the work [7,10,12,15], transformations plasticity are calculated as following:

$$\dot{\boldsymbol{\varepsilon}}^{tp} = \begin{cases} 0, & \text{for } \eta_k \le 0.03, \\ -3\sum_{k=2}^{k=5}(1-\eta_k)\varepsilon_{1k}^{ph}\dfrac{\mathbf{S}}{Y_1}\ln(\eta_k)\dot{\eta}_k, & \text{for } \eta_k \ge 0.03 \end{cases} \quad (17)$$

where $3\varepsilon_{1k}^{ph}$ are volumetric structural strains when the material is transformed from the initial phase „1" into the *k*-phase, Y_1 is a actual yield points of input phase (in cooling process it is austenite).

The equations (10) are solved by using the FEM [3,22]. The system of equations used for numerical calculation is:

$$[\mathbf{K}]\{\dot{\mathbf{U}}\} = \left(\{\dot{\mathbf{t}}^{Tph}\} - \{\dot{\mathbf{t}}^{e}\}\right) + \{\dot{\mathbf{t}}^{ptp}\} \quad (18)$$

where **K** is the element of stiffness matrix, **U** is the vector of nodal displacement, $\mathbf{t}^{Tph}$ is the vector of nodal forces resulting from thermal and structural strains, $\mathbf{t}^{e}$ is the vector of nodal forces resulting from the value change of Young's modulus dependent on the temperature, $\mathbf{t}^{ptp}$ is the vector of nodal forces resulting from plastic strains and transformation plasticity.

The final displacements, strains and stresses are resulting integration with respect to time, from initial $t=t_0$ (see (11)) to actual time *t*, i.e.

$$\mathbf{U}(x_\alpha,t) = \int_{t_0}^{t}\dot{\mathbf{U}}(x_\alpha,\tau)d\tau,\ \boldsymbol{\varepsilon}(x_\alpha,t) = \int_{t_0}^{t}\dot{\boldsymbol{\varepsilon}}(x_\alpha,\tau)d\tau,\ \boldsymbol{\sigma}(x_\alpha,t) = \int_{t_0}^{t}\dot{\boldsymbol{\sigma}}(x_\alpha,\tau)d\tau \quad (19)$$

The rate vectors of loads in the brackets in (17) are calculated only once in the increment of the load, whereas the vector $\mathbf{t}^{ptp}$ is modified in the iterative process.

In the numerical model the integrals (19) are approximate by following formula:

$$\begin{aligned} \mathbf{U}(x_\alpha,t^{s+1}) &= \sum_{k=0}^{k=s}\dot{\mathbf{U}}(x_\alpha,\Delta t^k)\Delta t^k + \dot{\mathbf{U}}^{Tph}(x_\alpha,\Delta t^{s+1})\Delta t^{s+1} + \sum_{it=1}^{mit}\delta^{it}\dot{\mathbf{U}}\Delta t^{s+1} \\ \boldsymbol{\varepsilon}(x_\alpha,t^{s+1}) &= \sum_{k=0}^{k=s}\dot{\boldsymbol{\varepsilon}}^{e}(x_\alpha,\Delta t^k)\Delta t^k + \dot{\boldsymbol{\varepsilon}}^{Tph}(x_\alpha,\Delta t^{s+1})\Delta t^{s+1} + \sum_{it=1}^{mit}\delta^{it}(\dot{\boldsymbol{\varepsilon}}^{p} + \dot{\boldsymbol{\varepsilon}}^{tp})\Delta t^{s+1} \\ \boldsymbol{\sigma}(x_\alpha,t^{s+1}) &= \sum_{k=0}^{k=s}\dot{\boldsymbol{\sigma}}(x_\alpha,\Delta t^k)\Delta t^k + \dot{\boldsymbol{\sigma}}(x_\alpha,\dot{\boldsymbol{\varepsilon}}^{Tph},\Delta t^{s+1})\Delta t^{s+1} + \sum_{it=1}^{mit}\delta^{it}\dot{\boldsymbol{\sigma}}(x_\alpha,\dot{\boldsymbol{\varepsilon}}^{ptp})\Delta t^{s+1} \end{aligned} \quad (20)$$

where *s+1* is the actual time step, *s* - previous time step, *mit* is the number of iteration in the increase of time Δt^{s+1}.

In the iterative process of evaluation of plastic strains, the modified Newton-Raphson algorithm is used [22,25].

5. Example of numerical calculations

The simulation of hardening process for axisymmetric element made of hot-work tool steel (W360) was performed. The dimension of the element was equal ϕ50×100 mm (Fig. 5).

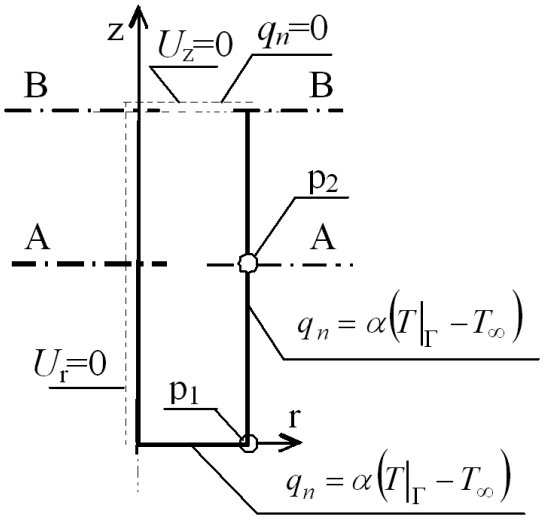

Fig. 5. The scheme of the considered object with boundary conditions

The initial temperature of hardened element was equal 300 K and the input structure was spheroidite. The element was heating in the fluidized bed with temperature 1600 K. The thermophysical coefficients *C* and λ were assumed as constants: 5.34×10^6 J/(m^{3}K) and 32 W/(mK). These are the average values calculated on the basis of the data in the work [14]. The heat transfer coefficient of the fluidized bed assumed constant (independent of temperature) and equal 2200 W/(m^{2}K). On the front surface of heated element the heat transfer coefficient had the value 1500 W/(m^{2}K). By using these values of coefficient the difficult (worse) flow around a fluidized bed on the front of surface of element was taken into account [26]. The simulation of heating was continuing to obtain the maximum temperature 1380 K in surroundings of point 1 (Fig. 5). The temperatures Ac_1 and Ac_3 in the phase transformations of heating (input structure - austenite) were equal 1033 and 1133 K appropriately (Fig. 1) [6]. The maximum temperature of the heating process was higher than Ac_3. It was connected with using in the simulation the CHT diagram with dynamic curves of start and finish of austenitization with taking into account the changes of range for austenite transformations for higher heating rate. These dynamic curves are higher than static temperatures Ac_1 and Ac_3 (see Fig. 2). In presented task the time of heating in the established conditions was equal 35 s, so the heating rate was ~30 K/s.

The obtained temperature distribution and austenite zone after finish of heating are presented in figure 6.

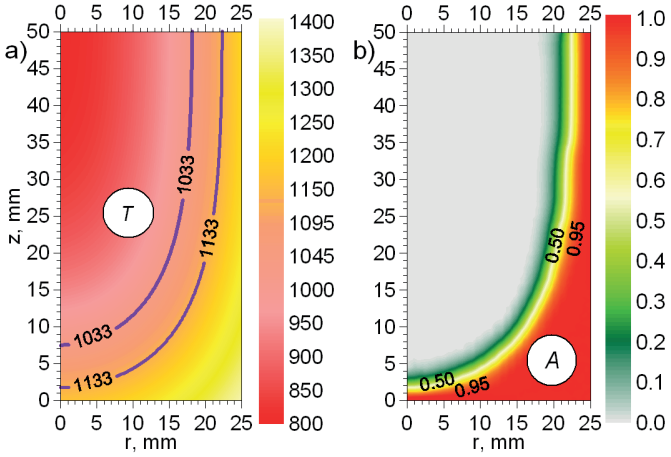

Fig. 6. Distributions of temperature a) and austenite b) after heating. Isolines with values 1033 and 1133 K, are the temperature of Ac_1 and Ac_3 appropriately. The area of austenite is less than in the case of using the dynamic curves $Ac_1(t)$ and $Ac_3(t)$ (CHT)

The cooling was modelled with the Newton condition and the value of heat transfer coefficient assumed equal 20 W/(m^{2}K) (cooling in the air [6,27]). The simulations of cooling process were performed for the two different sets of the boundary conditions. "Task 1": the temperature of coolant was constant and equalled T_∞=300 K. "Task 2": the temperature of surrounding medium (T_∞) was variable and taken the value on the level of 150 K less than average temperature of hardening element. When the average temperature of cooled element was below 450 K it was assumed that the temperature of coolant equalled 300 K. In the second task the cooling process was realized by using the constant heat flux with the value of 3000 W/m^2.

Hardened zones in the cross sections of the element, after cooling for both of task, are presented in figures 7, 8 and 9.

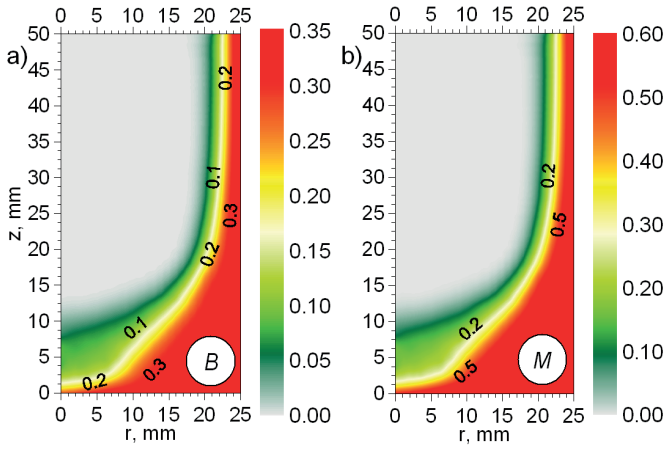

Fig. 7. Distributions of bainite a) and martensite b) after cooling (Task 1)

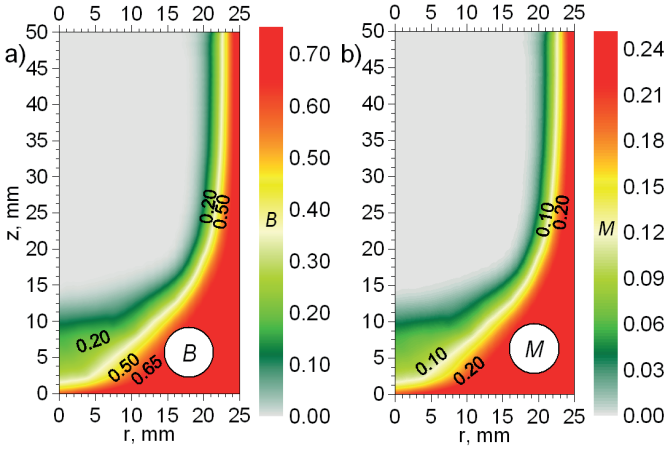

Fig. 8. Distributions of bainite a) and martensite b) after cooling (Task 2)

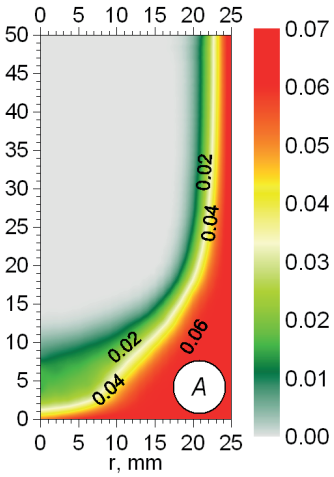

Fig. 9. Distributions of retained austenite after cooling (the results are comparable for both of task)

Distributions of the simulated fractions in the cross-section A-A (Fig. 5) after hardening are presented in figure 10.

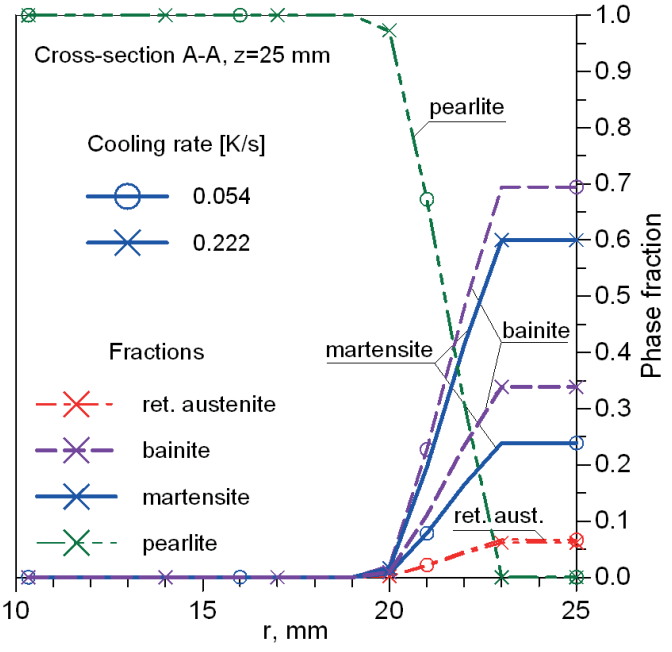

Fig. 10. Distribution of fractions along the radius (cross section A-A, Fig. 5). Comparison of results from two simulations

In the simulation on the mechanical phenomena the Young′s and tangent modulus (E and E^t) were dependent on temperature, whereas the yields stress (Y_0) was dependent on temperature and phase composition. Assumed, that Young′s and tangent modulus are equal 2×10^5 and 4×10^3 MPa (E^t=0.05E), yield points 150, 500, 1200 and 300 MPa for austenite, bainite, martensite and pearlite, respectively, in the temperature 300 K. In the temperature of solidus Young′s modulus and tangent modulus equalled 100 and 10 MPa, respectively, whereas yield points equalled 5 MPa. The discrete values of thermophysical properties depends on the temperature [3,13] were include by using the approximation with square spline functions (Fig. 11).

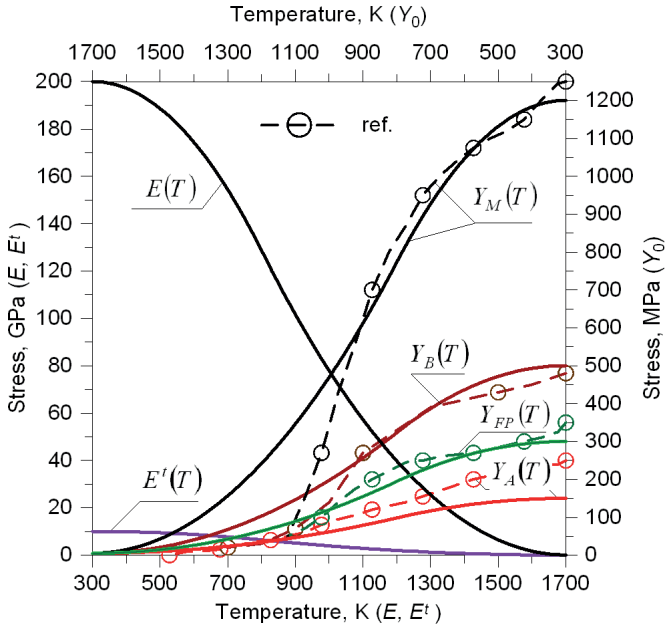

Fig. 11. The graph of the assumed functions of the material properties, depend on the temperature, used in model of stress: Young's modulus $E(T)$, tangent modulus $E_t(T)$ and yield point for each of phase $Y_0(T, \eta_k)$

The distributions of the residual stresses, after the hardening process were presented in the figures 12÷16. In the figures a) the results from the first task were shown, whereas in the figures b) from the second task.

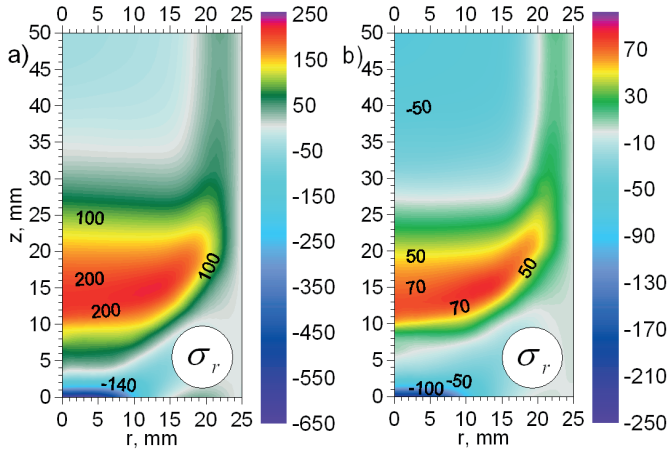

Fig. 12. Residual radial stresses, a) Task 1, b) Task 2

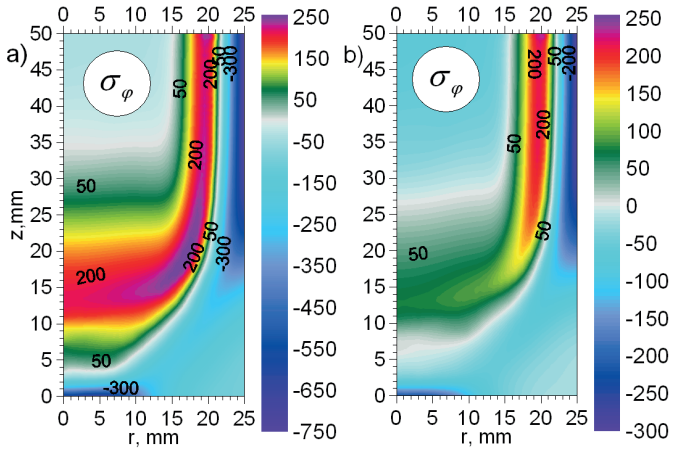

Fig. 13. Residual circumferential stresses, a) Task 1, b) Task 2

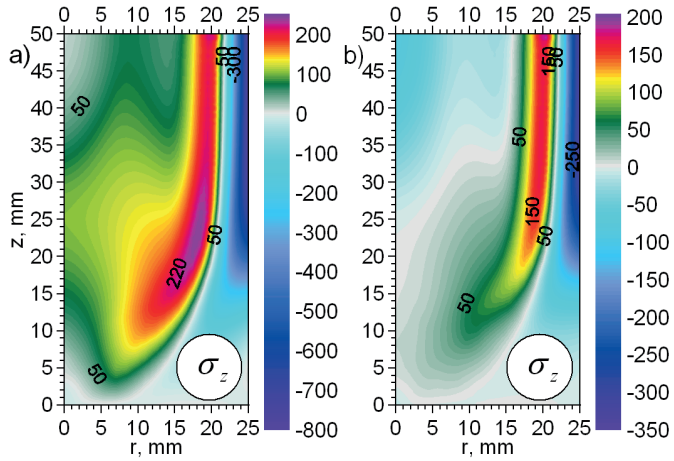

Fig. 14. Residual axial stresses, a) Task 1, b) Task 2

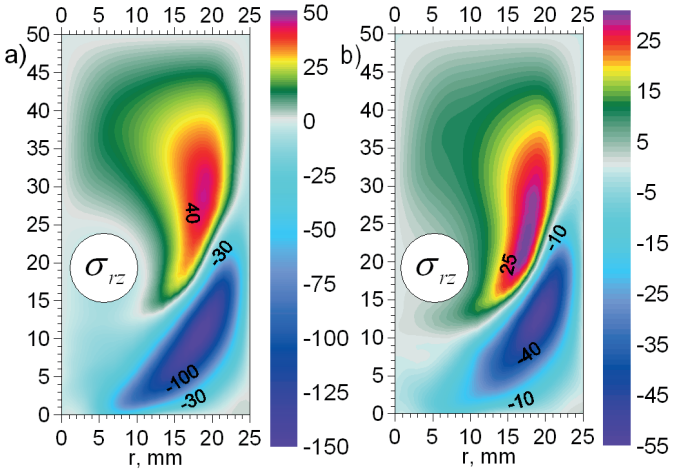

Fig. 15. Residual shear stresses, a) Task 1, b) Task 2

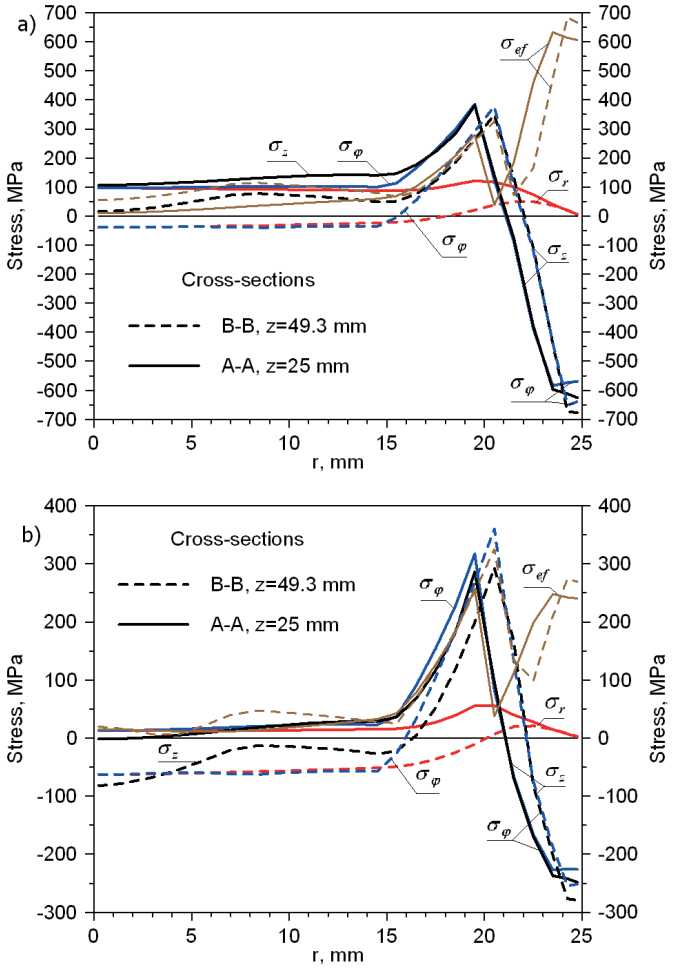

Fig. 16. Distributions of residual stresses in the cross sections B-B and A-A (Fig. 5), a) Task 1, b) Task 2

In the figure 17 the changes of stresses in the time of the hardening process in the superficial layer (point 2, Fig. 5) were presented.

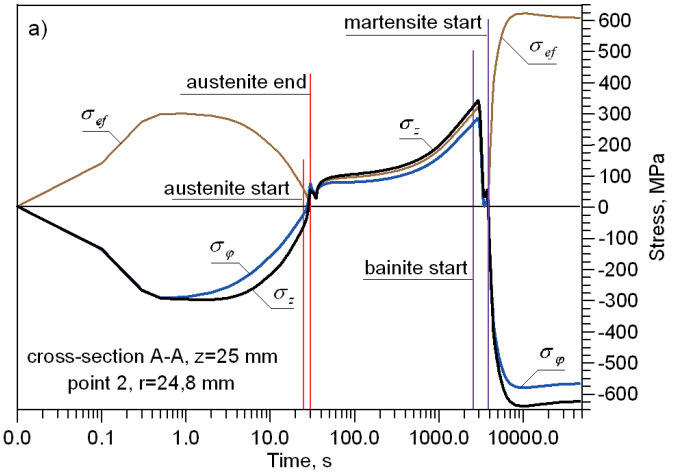

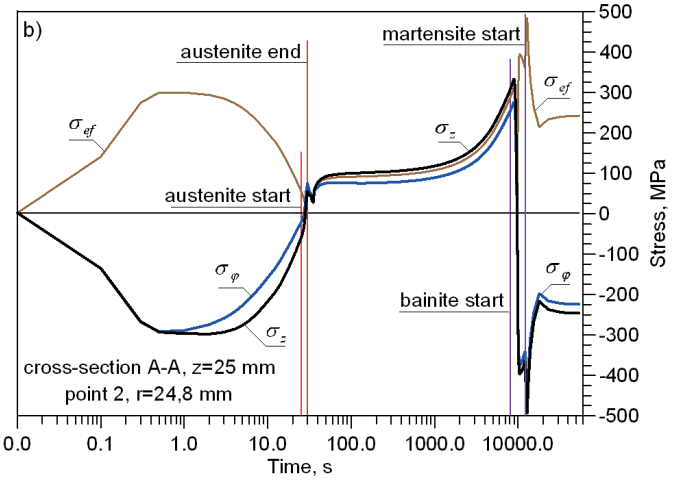

Fig. 17. The stresses according to the time (point 2, Fig. 5), a) Task 1, b) Task 2

The distributions (after the cooling process) of effective plastic strains were shown in the figure 18. Also the distributions of effective transformations induced plasticity were presented in the figure 19.

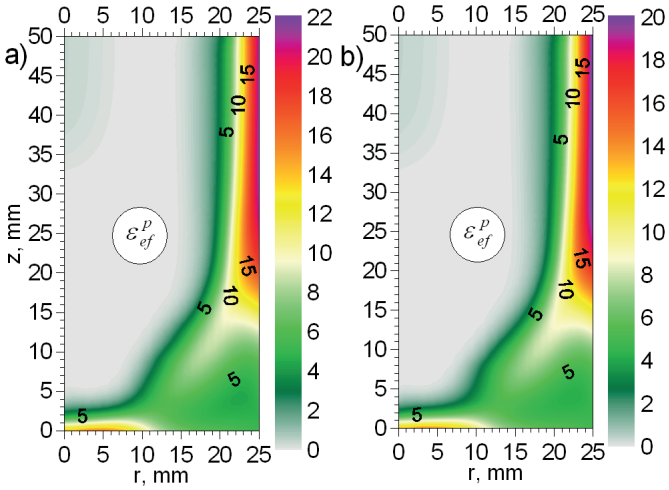

Fig. 18. The distributions of the effective plastic strains ($\times 10^{-3}$)

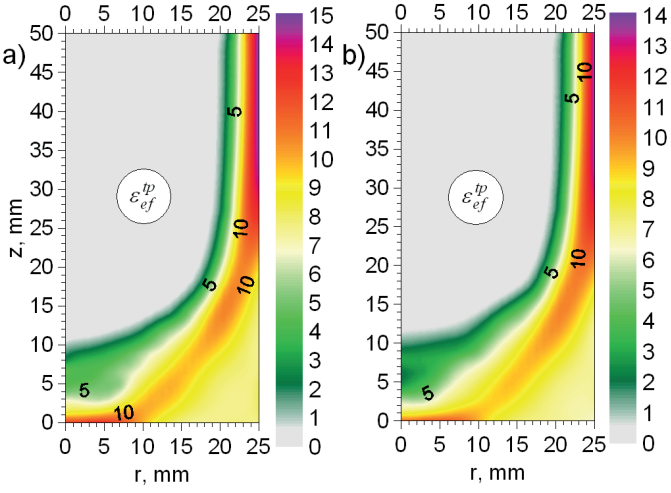

Fig. 19. The distributions of the transformations plasticity ($\times 10^{-3}$)

6. Conclusions

On the basis of simulated dilatometric curves can see that the considered steel is hardened very easy. To obtain the bainite-martensite structure the cooling rate can't be greater than 3.2 K/s (see Figs 1,2 and 3).

On the basis of obtained results from simulations of the superficial heat treatment can be concluded that the cooling in the heated air is much more preferred than in the air with room temperature. For these reasons, in the technology of hardening process of hot-work tool steel, the appropriate selection of the cooling rate is very important. The cooling in the air was applied and the cooling rate was equals: 0.234 and 0.222 K/s in the point 1 and 2 respectively "task 1" (Fig. 5). After the cooling process in the air the domination of martensite phase in structure of material is obtained (Figs 7 and 10). The cooling in the heated air was applied and the cooling rate was equals: 0.055 and 0.054 K/s in the point 1 and 2 respectively "task 2" (Fig. 5). After the cooling process in the heated air the domination of bainite phase in structure of material is obtained (Figs 8 and 10).

The distributions of the residual stress after the hardening process are more favorable for the example with the heated air. In the both tasks (1, 2) the circumferential and axial stresses are compressive, but after the cooling in the heated air the level of stresses in the second task is significantly lower (Figs 12÷15 and 16b). The deposition of compressive circumferential and axial stresses (the most meaningful stresses) is superficial (Figs 13, 14 and 16). The regular distributions of the stresses are obtained. Unfavorable is the distribution of shear stresses after the cooling process in the air with room temperature (Fig. 15a). The values of these stresses are much higher than the level of stresses obtained in second task. (see Fig. 15b). It can cause the cracking already in the hardening process.

It can be claimed that in the numerical simulation of such hardening the fact that transformation plasticity is included in the model of mechanical phenomena brings about the changes in obtained results [10,11,16]. The phase transformations significantly effect on the changes of the temporary stresses (Fig. 17) and in consequence on the residual stresses after hardening of the element considered.

The distributions of the effective plastic strains (Fig. 18) and effective transformations plasticity (Fig. 19) are comparable. Insignificantly differences in the solutions are occurred, but the area of distribution of strains is similar. It is independent on the type of cooling.

REFERENCES

[1] P. Carlone, G.S. Palazzo, Development and validation of a thermo-mechanical finite element model of the steel quenching process including solid-solid phase changes, International applied Mechanics **46**(8), 955-971 (2011).

[2] B. Chen, X.H. Peng, S.N. Nong, X.C. Liang, An incremental constitutive relationship incorporating phase transformation with the application to stress analysis, Journal of Materials Processing Technology **122**, 208-212 (2002).

[3] S.H. Kang, Y.T. Im, Three-dimensional thermo-elestic-plastic finite element modeling of quenching process of plain carbon steel in couple with phase transformation, International Journal of Mechanical Sciences **49**(4), 423-439 (2007).

[4] E.P. Silva, P.M.C.L. Pacheco, M.A. Savi, On the thermo-mechanical coupling in austenite-martensite phase transformation related to the quenching process, International Journal of Solids and Structures **41**, 1139-1155 (2004).

[5] R. Mahnken, A. Schneidt, S. Tschumak, H.J. Maier, On the simulation of austenite to bainite phase transformation, Computational Materials Science **50**, 1823-1829 (2011).

[6] Warmarbeitsstahl Hot Work Tool Steel, BOHLER W360, Iso Bloc, www.bohler-edelstahl.com

[7] S. Serejzadeh, Modeling of temperature history and phase transformation during cooling of steel, Journal of Processing Technology **146**, 311-317 (2004).

[8] Ch. Heming, H. Xieqing, W. Honggang, Calculation of the residual stress of a 45 steel cylinder with a non-linear surface heat-transfer coefficient including phase transformation during quenching, Journal of Materials Processing Technology **55**, 339-343 (1999).

[9] J.B. Leblond, J. Devaux, A new kinetic model for an isothermal metallurgical transformation in steel including effect of austenite grain size, Acta Materialia **52**, 137-146 (1984).

[10] A. Kulawik, A. Bokota, Modelling of heat treatment of steel with the movement of coolant Archives of Metallurgy and Materials, **56**(2), 345-357 (2011).

[11] C-H. Lee, K-H. Chang, Prediction of residual stresses in high strength carbon steel pipe weld considering solid-state phase transformation effects, Computers and Structures **89** (2011), 256-265.

[12] M. Cherkaoui, M. Berveiller, H. Sabar, Micromechanical modeling of martensitic transformation induced plasticity (TRIP) in austenitic single crystals, International Journal of Plasticity **14**(7), 597-626 (1998).

[13] M. Coret, A. Combescure, A mesomodel for the numerical simulation of the multiphasic behavior of materials under anisothermal loading (application to two low-carbon steels), International Journal of Mechanical Sciences **44**, 1947-1963 (2002).

[14] F. Fischer, G. Reinsner, E. Werner, K. Tanaka, G. Cailletaud, T. Antretter, A new view on transformation induced plasticity (TRIP), International Journal of Plasticity **16**, 723-748 (2000).

[15] L. Taleb, F. Sidoroff, A micromechanical modelling of the Greenwood-Johnson mechanism in transformation induced plasticity, International Journal of Plasticity **19**, 1821-1842 (2003).

[16] R.B. Pęcherski, Finite deformation plasticity with strain induced anisotropy and shear banding, Journal of Materials Processing Technology **60**, 35-44 (1996).

[17] C.H. Gür, A.E. Tekkaya, Numerical investigation of non-homogeneous plastic deformation in quenching process, Materials Science and Engineering **A 319-321**, 164–169 (2001).

[18] M. Dalgic, G. Löwisch, Transformation plasticity at different phase transformation of bearing steel, Mat.-wiss. u. Werkstofftech **37**(1), 122-127 (2006).

[19] L. Huiping, Z. Guoqun, N. Shanting, H. Chuanzhen, FEM simulation of quenching process and experimental verification of simulation results, Material Science and Engineering **A 452-453**, 705-714 (2007).

[20] D.Y. Ju, W.M. Zhang, Y. Zhang, Modeling and experimental

verification of martensitic transformation plastic behavior in carbon steel for quenching process, Materials Science and Engineering **A 438-440**, 246-250 (2006).

[21] K.J. Lee, Characteristics of heat generation during transformation in carbon steel, Scripta Materialia **40**, 735-742 (1999).

[22] O.C. Zienkiewicz, R.L. Taylor, The finite element method, Oxword: Butterworth-Heinemann, Fifth edition **1,2,3** (2000).

[23] M. Avrami, Kinetics of phase change, Journal of Chemical Physics, **I**(7), 1103-1112 (1939), **II**(8), 212-224 (1940), **III**(9), 117-184 (1941).

[24] D.P. Koistinen, R.E. Marburger, A general equation prescribing the extent of the austenite-martensite transformation in pure iron-carbon alloys and plain carbon steels, Acta Metallurgica 7, 59-60 (1959).

[25] S. Caddemi, J.B. Martin, Convergence of the Newton-Raphson algorithm in elastic-plastic incremental analysis, Int. J. Numer. Meth. Eng. **31**, 177-191 (1991).

[26] J. Jasiński, Influence of fluidized bed on diffusional processes of saturation of steel surface layer. Seria: Inżynieria Materiałowa Nr 6, Częstochowa (2003) (in Polish).

[27] H. Cheng, J. Xie, J. Li, Determination of surface heat-transfer coefficients of steel cylinder with phase transformation during gas quenching with high pressures, Computational Materials Science **29**, 453-458 (2004).

Received: 15 September 2015.